The new antitumor drug ABTL0812 inhibits Akt/mTORC1 axis by upregulating Tribbles-3 pseudokinase

Tatiana Erazo[1], Mar Lorente[2,3], Anna López[4], Pau Muñoz-Guardiola[1,5], Patricia Fernández-Nogueira[4], José A García-Martínez[5], Paloma Bragado[4], Gemma Fuster[4], María Salazar[2], Jordi Espadaler[5], Javier Hernández-Losa[6], Jose R Bayascas[7], Marc Cortal[5], Laura Vidal[8], Pedro Gascón[4,8], Mariana Gómez-Ferreria[5], José Alfón[5], Guillermo Velasco[2,3], Carles Domènech[5], Jose M Lizcano[1]

[1]Protein Kinases and Signal Transduction Laboratory, Institut de Neurociències and Departament de Bioquímica i Biologia Molecular, Universitat Autònoma de Barcelona, 08193 Bellaterra (Barcelona), Spain.

[2]Department of Biochemistry and Molecular Biology, Faculty of Biology, Universidad Complutense, Madrid, Spain.

[3]Instituto de Investigación Sanitaria del Hospital Clínico San Carlos (IdISSC), Madrid, Spain

[4]Area of Molecular and Translational Oncology, IDIBAPS, Fundació Clínic, Universitat de Barcelona, Barcelona, Spain.

[5]Ability Pharmaceuticals, SL, Edifici Eureka, Campus UAB, Bellaterra, Barcelona, Catalonia, Spain.

[6]Pathology Department, Hospital Universitari Vall d'Hebron, Barcelona, Spain.

[7]Institut de Neurociències and Department of Biochemistry and Molecular Biology, Universitat Autònoma de Barcelona, Barcelona, Spain.

[8]Medical Oncology Department, Novel Therapeutics Unit, Hospital Clínic Barcelona. Barcelona, Catalonia, Spain.

Corresponding author: Jose M Lizcano, Institut de Neurociències and Departament de Bioquímica i Biologia Molecular, Facultat de Medicina, Universitat Autònoma de Barcelona, 08193 Bellaterra (Barcelona), Spain

Email: josemiguel.lizcano@uab.es

Phone: +34 935 813 076 Fax: +34 935 811 573

Running title: Inhibition of Akt/mTORC1 axis by TRIB3 pseudokinase

Keywords: Akt inhibition, Tribbles-3, autophagy, small compound, PPAR peroxisome proliferator-activated receptor

Financial Support.

This work was supported by grants from the Government of Catalonia (ACCIO/FINEBT10-1-0047), and from the Spanish Ministry of Economy and Competitiveness (MINECO), (CDTI/PID/IDI-20101630, Genoma España/INNOCASH/2011196, ENISA/EBT2012/100375, INNPACTO/IPT-2012-0614-010000. J.A. and M.G-F were funded by Torres-Quevedo grant (MINECO), and M.C. by an Inncorpora grant (MINECO). Work in G Velasco's laboratory was supported by grants from Spanish Ministry of Economy and Competitiveness (MINECO), FEDER (PI12/02248) and Fundación Mutua Madrileña (AP101042012).

Disclosure of Potential Conflicts of Interest.

Jose M Lizcano and Pedro Gascón are advisory members of Ability Pharmaceuticals SL.

Statement of translational relevance

Hyperactivation of the Akt/mTORC1 axis is commonly observed in many human cancers and blocking this pathway is an important anticancer strategy. Inhibition of Akt is a valid target for anticancer therapy and several AKT inhibitors are under clinical development. We present ABTL0812, a first-in-class small molecule with a unique mechanism of action. In cells and tumor xenografts models, ABTL0812 induces upregulation of TRIB3 pseudokinase. TRIB3 binds Akt, preventing its activation by upstream kinases and resulting in an effective inhibition of the Akt/mTORC1 axis and in autophagy-mediated cancer cell death. ABTL0812 is currently in Phase I/Ib First-in-Human Clinical Trial in patients with advance solid tumors. Preliminary results show that ABTL0812 also induces Akt inhibition in humans. These evidences, together with a very low toxicity and high tolerability, support further development of ABTL0812.

Word counting. Introduction, Results, Discussion, Methods & Figure legend Sections: 4979 words.

Number of Figures and Tables: 6 Figures

Number of Supplementary Figures and Tables: 7 supplementary Figures; 1 Supplementary Table

Abstract

Purpose: ABTL0812 is a novel first-in-class, small molecule which showed anti-proliferative effect on tumor cells in phenotypic assays. Here we describe the mechanism of action of this antitumor drug, which is currently in clinical development.

Experimental design: We investigated the effect of ABTL0812 on cancer cell death, proliferation and modulation of intracellular signaling pathways, using human lung (A549) and pancreatic (MiaPaCa-2) cancer cells and tumor xenografts. To identify cellular targets, we performed *in silico* high throughput screening comparing ABTL0812 chemical structure against ChEMBL15 database.

Results: ABTL0812 inhibited Akt/mTORC1 axis, resulting in impaired cancer cell proliferation and autophagy-mediated cell death. *In silico* screening led us to identify Peroxisome Proliferator-Activated Receptors PPARα and PPARγ as the cellular targets of ABTL0812. We showed that ABTL0812 activates both PPAR receptors, resulting in upregulation of Tribbles-3 pseudokinase (TRIB3) gene expression. Upregulated TRIB3 binds cellular Akt, preventing its activation by upstream kinases, resulting in Akt inhibition and suppression of the Akt/mTORC1 axis. Pharmacological inhibition of PPARα/γ or TRIB3 silencing prevented ABTL0812-induced cell death. ABTL0812 treatment induced Akt inhibition in cancer cells, tumor xenografts and PBMCs from patients enrolled in Phase I/Ib First-in-Human Clinical Trial.

Conclusions: ABTL0812 has a unique and novel mechanism of action, that defines a new and drugable cellular route that links PPARs to Akt/mTORC1 axis, where TRIB3 pseudokinase plays a central role. Activation of this route (PPARα/γ-TRIB3-Akt-mTORC1) leads to autophagy-mediated cancer cell death. Given the low toxicity and high tolerability of ABTL0812, our results support further development of ABTL0812 as a promising anticancer therapy.

Introduction

The phosphatidylinositol 3-kinase (PI3K)/AKT/mTORC1 (mTOR Complex-1) signaling pathway drives signals from ligand-stimulated receptor tyrosine kinases (RTK) to proteins that control cell metabolism, growth, size, survival and angiogenesis (1). In response to growth or survival factors, phosphorylated RTKs activate PI3K, which generates the phosphatidylinositol 3,4,5-trisphosphate (PIP3) second messenger and allows the recruitment of protein kinase Akt to the cellular membrane. Akt binds PIP3 through its PH domain, resulting in a conformational change that enables its activation through phosphorylation of two critical residues: Thr308 at the T-loop of the kinase domain by the phosphoinositide-dependent kinase-1 (PDK1), and Ser473 at the C-terminal hydrophobic motif by mTOR complex-2 (mTORC2) (2, 3). Active Akt phosphorylates a plethora of substrates that regulate cell survival and metabolism, and also cell growth through subsequent activation of mTORC1. Akt phosphorylation of PRAS40 and TSC2 leads to activation of mTORC1, which promotes protein translation and synthesis by phosphorylating ribosomal S6-Kinase (S6K) and the elongation factor 4EBP-1 (4).

Human cancer is very often associated with activation of the PI3K/Akt/mTORC1 pathway, mainly due to overexpression or activating mutations of RTKs and PI3K, to deletions/mutations of the PIP3 phosphatase PTEN and to amplification of Akt (3,5). These types of tumors are hypersensitive to inhibition of each of the components of the PI3K/Akt/mTORC1 axis, and therefore major efforts have been taken to develop inhibitors of this signaling pathway (6). Akt acts as a central node of this pathway, and hyperactivated Akt is a common feature observed in human solid tumors (3,5). Therefore, Akt has been proposed as an interesting target in cancer therapy. Two classes of Akt inhibitors are now in clinical development: ATP-competitive inhibitors (such as GSK690693) which target active Akt, and allosteric inhibitors (such as MK-2206 and perifosine, currently in Phase II and Phase III clinical trials, respectively) that by binding the PH domain of Akt prevent its activation by upstream kinases (3,7).

Here we present ABTL0812, a first-in-class molecule with antitumor activity which is currently in Phase I/Ib clinical trials in patients with advanced solid tumors. We provide evidences showing that ABTL0812 inhibits Akt phosphorylation by upregulating the expression of TRIB3, a pseudokinase that binds and inhibits Akt, leading to mTORC1 inhibition and autophagy-mediated cell death.

Methods

Cell culture, viability assay, transfection and lysis. Human cancer cell lines were purchased from American Type Culture Collection (2008; ATCC-authentication by isoenzymes analysis). $Atg5^{+/+}$ and $Atg5^{-/-}$ T-large antigen-transformed MEFs were donated by Dr. Mizushima (Tokyo Medical University, Japan). $TRB3^{+/+}$ and $TRB3^{-/-}$ RasV12/E1A-transformed MEFs have been described before (8). Cell lines were cultured as recommended and transfected using Lipofectamine-2000. Cell viability was determined by the MTT assay (9). Cells were lysed in ice-cold RIPA buffer supplemented with 1mM sodium-orthovanadate, 50mM NaF and 5mM sodium-pyrophosphate, sonicated and stored at -20°C.

Immunoblotting and immunoprecipitation. Immunoblot analyses were performed following standard procedures as described (10) and antibodies listed in the Supplementary Table 1. Akt was immunoprecipitated following the protocol previously described (11).

Transmission Electron Microscopy. Cells treated with ABTL0812 or vehicle (ethanol) were processed as described before (12). Pellets were embedded in Eponate-12TM resin (Ted Pella). Ultrathin (70nm-thick) sections were contrasted with uranyl-acetate and lead citrate solutions, and visualized in transmission electron microscope (Jeol JEM-1400) equipped with a CCD- GATAN-ES1000W Erlangshen camera.

Xenograft models. For A549 model, athymic female nude mice (n=5 per group) were injected subcutaneously with $5x10^6$ cells in each flank. When tumors reached 80-100 mm^3, mice were randomly distributed into treatment groups and administered the corresponding treatments. ABTL0812 was administered by oral gavage at 120 mg/kg every day. Docetaxel was administered by intraperitoneal route at 15mg/kg once a week. MiaPaCa-2 cells were injected in athymic male mice (n=5 per group) with $10x10^6$ cells in one flank. When tumors reached 80-160 mm^3, mice were randomly distributed and treated with vehicle or ABTL0812 120mg/kg by oral gavage five times per week. Tumor volumes were measured as (length x $width^2$)/2 twice a week. All procedures involving animal were performed with the approval of the Hospital Clinic Animal Experimentation Committee, according to Spanish official regulations.

Pharmacokinetics of ABTL0812 in mice and rats. ABTL0812 was orally (gavage, 100 mg/kg) and intravenously (10 mg/kg) administered to male CD-1 mice. ABTL0812 was quantified in plasma by validated LC-MS/MS methods, and pharmacokinetic parameters were calculated with WinNonlin software.

Clinical Trial and isolation of PBMC from patients. ABTL0812 is currently in clinical evaluation in a Phase I/Ib trial in patients with advanced solid tumors. This study was approved by the local Ethics Committee of the Hospital Clinic Barcelona and the Spanish Agency of Medicines. The trial is registered at www.clinicaltrials.gov (NCT02201823). ABTL0812 was administered daily by the oral route at a dose of 1000 mg bid for a period of 28 days. Blood samples for biomarker study were obtained by venepuncture before and after ABTL0812 treatment. PBMC were isolated by Ficoll (GE-Healthcare) density centrifugation, lysed in RIPA buffer, sonicated and stored at -20°C.

Statistical analysis. All in vitro data were assessed using one-way analysis of variance (ANOVA) followed by Bonferroni's multiple comparison test. Tumor volumes of mice were compared using the ANOVA followed by t-test. Statistical significance between the groups was assessed with the log-rank test (GraphPad). Levels of statistical significance were set at $P \leq 0.05$.

Results

ABTL0812 has anticancer activity *in vitro* and *in vivo*

A novel class of chemically modified lipid-derived small molecules was selected based on two phenotypic assays: anti-proliferative effect on tumor cells and low toxicity after high doses administration in rodents. From this class, ABTL0812 was selected for further preclinical development. ABTL0812 formula is 2-hydroxylinoleic acid (Fig. 1A).

ABTL0812 reduced viability of different human cancer cell lines tested with IC_{50} values of 20-60 μM (Fig. 1B). Real time cell analyses further demonstrated the antiproliferative effect of ABTL0812 (Supplementary Fig. S1). ABTL0812 also induced cell death, which was confirmed by propidium iodide staining (Supplementary Fig. S2). Importantly, ABTL0812 induced death in cancer cells but not in normal cells. Compared to LN-18 gliobastoma cells, primary astrocytes were resistant to ABTL0812 treatment at the highest ABTL0812 concentration tested (200 μM) (Fig. 1C).

To address ABTL0812 pharmacokinetics, we administered the compound to mice by oral and intravenous routes. ABTL0812 showed an excellent bioavailability by oral route (F:103%), with rapid oral absorption (t_{max}:30 min), high pick concentrations (C_{max}:2.0 μg/mL) and wide volume of distribution (Vss:10.4 L/kg). Clearance was also high (Cl: 82 mL/min/kg). Overall, the compound was well tolerated and animals appeared healthy with no clinical signs of distress, local or systemic toxicity.

To test the efficacy of ABTL0812 in inhibiting tumor growth *in vivo* we used human lung and pancreatic xenograft models. A549 human lung cancer xenografts of nude mice were treated with ABTL0812 or the standard of care docetaxel. ABTL0812 inhibited tumor progression with an efficacy similar to docetaxel (Fig. 1D). Moreover, ABTL0812 lacked the toxic effects observed for docetaxel, as shown by body weight measurements. Similarly, ABTL0812 also inhibited the growth of MiaPaCa-2 human pancreatic cancer xenografts in nude mice, without affecting body weight (Fig. 1E).

ABTL0812 induces autophagy-mediated cell death

Next, we investigated the type of cell death induced by ABTL0812 in A549 and MiaPaCa-2 cells. ABTL0812 did not induce nuclear fragmentation/condensation, or caspase-3 activation (Supplementary Fig. S3). Treatment with staurosporine resulted in typical features of apoptosis, showing that A549 and MiaPaCa-2 cells are apoptosis-competent. These results indicate that ABTL0812 fails to induce apoptosis. In turn, several evidences indicated that ABTL0812-induced cell death is mediated by autophagy.

Two of the hallmarks of autophagy are the conversion of the soluble form of LC3 to a lipidated form associated to autophagosomes (LC3-II), and the elimination of autophagosome cargo proteins such as p62 (13). In A549 and MiaPaCa-2 cells, ABTL0812 induced the appearance of LC3-II and a decrease on p62 protein in a concentration-dependent manner (Fig. 2A). We also observed the occurrence of LC3-positive dots in cells treated with ABTL0812, which indicates association to autophagosomes (Supplementary Fig. 4). Electron microscopy analysis of ABTL0812-treated A549 and MiaPaCa-2 cells revealed the presence of double membrane vacuolar structures with the morphological features of autophagosomes (Fig. 2B). Moreover, ABTL0812 also induced hallmarks of autophagy *in vivo*, since tumors from A549 xenograft mice treated with ABTL0812 showed an increase in LC3-II levels, compared with mice treated with vehicle (Fig. 2C).

Next, we investigated the role of autophagy in the cell death induced by ABTL0812. Pharmacological inhibition of autophagy was achieved by treating cells with a combination of the lysosomal protease inhibitors E64d and Pepstatin-A (PA) that block the final step of autolysosomal degradation. Treatment of cells with E64d+PA prevented ABTL0812-induced cell death and resulted in an enhancement of LC3-II accumulation in cells treated with ABTL0812 (Fig. 2D), indicating that ABTL0812 induces dynamic autophagy in cancer cells. Finally, we evaluated the activity of ABTL0812 in oncogene-transformed embryonic fibroblasts derived from $Atg5^{-/-}$ (autophagy-deficient) mice. Atg5 is an essential protein for autophagosome formation (14). Transformed $Atg5^{-/-}$ MEF cells were more resistant to ABTL0812-induced cell death than transformed $Atg5^{+/+}$ MEF cells, and did not activate autophagy in response to ABTL0812 treatment (Fig. 2E). Taken together, these results show that autophagy mediates ABTL0812-induced cancer cell death.

ABTL0812 inhibits the Akt/mTOR axis

Autophagy induction is often consequential to the inhibition of mTOR signaling, since mTORC1 acts as a central regulator in autophagy induction (15). We therefore investigated whether ABTL0812-induced autophagy and cancer cell death occurred via mTORC1 inhibition, by measuring levels of activation of components of the Akt/mTORC1 signaling pathway. A549 and MiaPaCa-2 cells showed measurable phosphorylation levels for all the proteins of Akt/mTORC1 axis in basal conditions. ABTL0812 treatment reduced phosphorylation of ribosomal-S6 kinase and of ribosomal-S6 protein (a well-established S6K substrate) in a concentration-dependent manner (Fig. 3).

Protein kinase Akt modulates the activation of mTORC1 by phosphorylating and inactivating the

TSC2 and PRAS40 proteins that act as repressors of mTORC1 activity (1). Thus, Akt inhibition results in impaired mTORC1 activity and activation of autophagy. ABTL0812 induced Akt inhibition in A549 and MiaPaCa-2 cells in a dose dependent manner, by reducing phosphorylation of the two critical residues involved in Akt activation, Thr308 and Ser473. Consequently, ABTL0812 also reduced phosphorylation of the Akt substrates PRAS40 and TSC2 (Fig. 3). These results show that ABTL0812 induced inhibition of the Akt-mTORC1 axis in cancer cells.

ABTL0812 binds and induces PPARα and PPARγ transcriptional activities, which mediate in ABTL0812-induced cancer cell death

To identify the molecular targets of ABTL0812, we performed *in silico* high throughput screening comparing ABTL0812 chemical structure against the ChEMBL15 database (https://www.ebi.ac.uk/chembldb/), following the *similar property* and *active analog* principles (16). This approach allowed the identification of several ABTL0812 target candidates, including PPARα and PPARγ (peroxisome proliferator-activated receptors alpha and gamma). Of note, a possible interaction with PPARβ/δ was not found. Putative ABTL0812-binding molecules identified in this screening were further investigated through docking analysis. Fig. 4A shows the molecular model of ABTL0812 into the ligand binding pocket of PPARγ. In this model, ABTL0812 may bind the PPARγ ligand binding domain (LBD) through its carboxylate group, which forms hydrogen bonds with the side of key amino acid residues (Ser289, His323, Tyr473 and His449), as it has been shown for other PPARγ agonists such as rosiglitazone (17). The 2-hydroxyl group of ABTL0812 may also form hydrogen bonds with residues Cys285 and Ser289, which are also conserved in the PPARα LBD. This molecular model proposes that ABTL0812 might establish interactions similar to the specific PPARγ agonist rosiglitazone, thus predicting that ABTL0812 could act as PPAR agonist. Indeed, *in vitro* radioligand displacement assays using purified proteins showed that ABTL0812 binds PPARα and PPARγ ligand-binding pockets with K_i values of 7.1 μM and 4.7 μM, respectively (Supplementary Fig. S5).

Next, we investigated the functional relevance of this interaction, performing luciferase-based gene reporter assays in cells transfected with a PPAR-response element (PPRE) fused to luciferase construct. In A549 and MiaPaCa-2, ABTL0812 induced ~5 fold PPAR transcriptional activity, similarly to the specific agonists WY-14643 (PPARα) or rosiglitazone (PPARγ) (Supplementary Fig. S6). To determine if ABTL0812-induced PPAR activation was mediated by the PPAR isoforms alpha and/or gamma, we performed analogous gene reporter assays in cells transiently transfected with plasmids encoding each isoform. ABTL0812-induced PPAR transcriptional activity was higher in cells over-expressing PPARα or PPARγ proteins, compared with those having the endogenous

proteins only (Fig. 4B), suggesting that ABTL0812 functionally interacts with both receptors in cells.

Finally, we performed cell viability assays in the presence of PPARα/γ antagonists. In A549 and MiaPaCa-2 cells, pre-incubation with PPARα antagonist GW6471 or PPARγ antagonist GW9662 prevented cell death induced by ABTL0812 (Fig. 4C), indicating that PPAR receptors mediate in ABTL0812-induced cell death.

ABTL0812 activates PPARα- and PPARγ-dependent expression of TRIB3

Koo et al. showed that PPARs regulate the expression of the pseudokinase Tribbles 3 (TRIB3), through binding a PPAR responsive element sequence within the TRIB3 promoter (18). Other authors have shown that TRIB3 can interact with Akt, preventing its activation by upstream kinases and resulting in an inactive form of Akt (8,19). Thus, we hypothesized that ABTL0812 could inhibit Akt (and downstream mTORC1) by upregulating TRIB3 via PPARα/γ activation. In A549 and MiaPaCa-2 cells, ABTL0812 induced a quick and robust increase in TRIB3 protein levels after 12 h of treatment (Fig. 5A), that correlated with an increase in gene transcription (Fig. 5B) and qPCR-measured TRIB3 mRNA levels (Fig. 5C). Although we cannot discard an effect of ABTL0812 on TRIB3 stability, these results indicate that ABTL0812 upregulates TRIB3 gene transcription. Furthermore, treatment with PPARα and/or PPARγ inhibitors GW6471 and GW9662, respectively, completely abolished the ABTL0812-induced upregulation of TRIB3 gene expression (Fig. 5C). Interestingly, treatment with either PPARα or PPARγ agonists resulted in increased TRIB3 expression and reduced Akt phosphorylation (Fig. 5D). However, it was necessary a combined treatment with both agonists to obtain similar levels of inhibition of Akt (phospho-PRAS40) and mTORC1 activities (phospho-S6K and phospho-S6) than those induced by ABTL0812. Altogether, our results demonstrate that ABTL0812 induces TRIB3 gene expression via activation of PPARα and PPARγ activities.

ABTL0812 inhibits Akt and mTORC1 via TRIB3

To investigate the role of upregulated TRIB3 on Akt activation, we overexpressed increasing amounts of TRIB3 in A549 and MiaPaCa-2 cells. We observed reduced phosphorylation of Akt and Akt substrate PRAS40 that inversely correlated with TRIB3 expression (Fig. 6A). This was probably due to a TRIB3-Akt physical interaction, since ABTL0812 treatment increased the amount of Akt co-immunoprecipitated with TRIB3 (Fig. 6B). Moreover, unlike wild type transformed MEF, TRIB3 deficient MEF cells did not show Akt (Ser473) or mTORC1 (pS6) inhibition, or induction of autophagy (LC3-II marker) in response to ABTL0812 treatment (Fig. 6C). Cell viability assays

showed that TRIB3 deficient MEFs are resistant to ABTL0812-induced cell death, unlike wild type transformed MEFs (Fig. 6D). These results support a pivotal role of TRIB3 on the impairment of the Akt/mTORC1 axis and on the autophagy-mediated cancer cell death observed in response to ABTL0812 treatment.

ABTL0812 induces TRIB3 upregulation and Akt inhibition *in vivo*

To determine the *in vivo* relevance of our findings, we next investigated the effect of ABTL0812 in A549 human lung and MiaPaCa-2 human pancreatic cancer xenografted mice (Fig. 1C-D). Immnuohistochemical and immunoblotting analyses showed that ABTL0812 induced upregulation of TRIB3 protein and inhibition of Akt phosphorylation (Ser473) in A549 and MiaPaCa-2 tumors (Fig. 6E). These data, together with that presented in Fig. 2 showing that ABTL0812 induces autophagy in A549 xenografts, suggest that the antitumor activity of ABTL0812 *in vivo* relies on inhibition of Akt and induction of autophagy-mediated cell death.

Akt phosphorylation is a pharmacodynamic marker in patients treated with ABTL0812

Finally, we evaluated the activity of ABTL0812 in some patients included in Phase I/Ib clinical trials (NCT02201823), monitoring Akt phosphorylation levels in peripheral blood mononuclear cells (PBMC). We collected blood samples, pre-treatment and at different days of chronic treatment with 1000mg of ABTL0812, a dose that was safe and well tolerated (preliminary data not shown). Our preliminary results show that treatment with ABTL0812 resulted in a marked reduction on Akt phosphorylation in PBMCs from three patients (Fig. 6F)**.** We could not detect TRIB3 protein in PBMCs, using commercially available anti-TRIB3 antibodies. However, parallel qPCR analysis showed a significant increase in TRIB3 mRNA levels in human PBMCs treated *in vitro* with ABTL0812 (Supplementary Fig. S7), thus suggesting that ABTL0812 also induces Akt inhibition in humans through upregulation of TRIB3.

Discussion

Here we present the mechanism of action of ABTL0812, a novel and first-in-class antitumor drug which is currently in Phase I/Ib clinical trials in patients with advanced solid tumors. ABTL0812 is a polyunsaturated fatty acid derivative, small molecule that induces cell death in a broad panel of cancer cell lines, whereas it does not affect cell viability of non-tumorogenic cells. ABTL0812 also inhibits tumor growth in human lung and pancreatic tumor xenografts. Herein, we elucidated a novel cell signaling pathway through which ABTL0812 induces autophagic cell death. We showed that ABTL0812 induces upregulation of the TRIB3 pseudokinase through activation of PPARα and PPARγ transcription factors. Upregulated TRIB3 binds to Akt and prevents its activation by PDK1 and mTORC2 upstream kinases, resulting in inhibition of the Akt/mTORC1 axis and, therefore autophagy-mediated cell death (Fig. 6G).

Autophagy is an essential process that consists of selective degradation of cellular components, assuring the maintenance of cellular homeostasis via lysosomal degradation pathways (13). The role of autophagy in cancer is still far from clear, as it can act as a tumor suppressor and tumor promoter, depending on tumor type, stage and genetic context, as well as on the duration and strength of the triggering stimuli (15,20). Our results demonstrate that ABTL0812 induces autophagy-mediated cancer cell death *in vitro* and *in vivo*, without activating cellular apoptosis**.** These results are in agreement with those reporting that polyunsaturated fatty acid and derivatives exert their anti-proliferative action through activation of autophagy (21-23).

The majority of current anticancer treatments activate apoptosis, and resistance to chemotherapy is a major challenge in cancer (24). Autophagy-mediated cell death has emerged as an alternative to kill cancer cells without inducing resistance to apoptosis inducer drugs (25). mTORC1 plays a central role in regulating cellular autophagy, and mTORC1 inhibitors induce autophagy-mediated cell death in many systems, such as AZD8055 in hepatocellular carcinoma (26) or Ku0063794 and temsirolimus in renal carcinoma (27). On the other hand, mTORC1 activation is frequently associated with resistance to antitumor drugs (6). Since ABTL0812 is a potent inhibitor of the Akt/mTORC1 axis, its administration in combination with standard chemotherapeutic drugs might prove effective in therapy-resistant or apoptosis-refractory tumor. This has been shown for the mTORC1 inhibitor everolimus (RAD001), which sensitizes papillary thyroid cancer cells to treatment with doxorubicin by an autophagy-mediated mechanism (28).

Here we present *in vitro* and *in vivo* evidences showing that ABTL0812 binds to and activates PPARα and PPARγ transcriptional activities, and that pharmacological inhibition of both receptors prevents ABTL0812-induced cancer cell death, suggesting that PPARα/γ are the primary molecular

targets of ABTL0812 in the cell. PPARs are nuclear receptors that heterodimerize with the retinoid-X receptors to modulate gene transcription. Mammalian cell express three PPAR isoforms, PPARα, PPARβ/δ, and PPARγ (29). Using an *in silico* analysis, we identified PPARα and PPARγ as targets of ABTL0812, but not PPARβ/δ. Several authors have shown that polyunsaturated and derivative long fatty acid activate PPARs transcriptional activities (21,30). Interestingly, the docking experiments performed in our study show that the alpha hydroxyl group in ABTL0812 forms two extra hydrogen bonds with the critical residues Cys285/Ser289 in PPARγ LBD (also conserved in the PPARα LBD) , compared with the non-hydroxylated linoleic acid. Accordingly, ABTL0812 showed higher PPARγ agonistic activity (Ki ~5 μM) than linoleate (79 μM) or the PPARγ natural agonists flavonoids such as kaempferol (30 μM) (30).

PPARs regulate the expression of many genes involved in glucose and lipid metabolism (29,31). Interestingly, activation of PPARγ reduces cell proliferation and invasion, and enhances apoptosis in different cancer models such as breast and hepatocarcinoma (21,32), whereas activation of PPARα inhibits tumor growth and angiogenesis in mouse models (33-35). Therefore, activators of PPARα or PPARγ have been proposed as anti-cancer drugs, and specific synthetic PPARα or PPARγ agonists are in clinical trials for treating cancer, such as the PPARγ agonist efatutazone or the PPARα agonist fenofibrate, in patients with liposarcoma (NTC02249949) or multiple myeloma (NCT01965834), respectively. ABTL0812, by activating PPARα and PPARγ, might well synergize the anti-cancer activity of each receptor. Importantly, single treatment of the cancer cells used in our study with either PPARα or PPARγ agonist induced partial inhibition of mTORC1 activity, whereas combined treatment with both agonists resulted in a robust mTORC1 inhibition, similar to that obtained for ABTL0812 treatment (Fig. 5D). Given the fact that a new generation of dual PPARα/γ agonists has shown promising anti-cancer activity (i.e. TZD18 in breast cancer, 36), it will be of interest to investigate if PPARα/γ mechanism of action also involves inhibition of the Akt/mTORC1 axis.

Our most striking result is the observation that upregulation of Tribbles pseudokinase-3, through activation of PPARα/γ receptors, plays a crucial role in the anti-cancer activity of ABTL0812. TRIB3 is a highly conserved protein which lacks critical catalytic residues for binding ATP and therefore lacks kinase activity (37). Together with TRIB1 and TRIB2 proteins, TRIB3 define the Tribbles subfamily of pseudokinases, which was first described in *Drosophila* as regulators of cell proliferation and migration during development (38). As it happens for other pseudokinases, TRIB3 exerts its function in the cell interacting with several proteins, such as the transcription factors SMAD3 (39) and ATF-4 (40), or members of the MAPK family (41). Of note, few authors have shown that TRIB3 can interact with Akt, preventing its phosphorylation by upstream kinases

and resulting in suppression of the insulin pathway (16,19,42). Here we show that ABTL0812-evoked TRIB3 binds Akt, and that TRIB3 overexpression in cells resulted in Akt inhibition. Moreover, we also found that treatment with ABTL0812 enhances the interaction between TRIB3 and Akt, in line with previous data obtained in glioma cells and oncogene-transformed MEFs, where a similar increase in TRIB3 levels and TRIB3-Akt interaction occur upon exposure to Δ^9-tetrahydrocannabinol (THC, 12). TRIB3 interacts more strongly with inactive/dephosphorylated Akt than active Akt (M. S., unpublished results), therefore it is likely that overexpressed TRIB3 could trap the inactive form of Akt, preventing its activation/phosphorylation by upstream kinases. Whether TRIB3 masks the phosphorylatable residues in Akt (Thr308 and Ser473), induces a conformational change that impairs recognition by upstream kinases PDK1 and mTORC2, or hampers the binding of the Akt PH domain to PIP3 remains to be clarified. On the other hand, it is also likely that, in addition to changes in TRIB3 protein levels, there could exist additional mechanisms involved in regulating the interaction of TRIB3 with its protein targets, and specifically with Akt. Posttranslational modifications of TRIB3 – yet to be described-, and/or changes in the interaction with other members of the Tribbles family that participate in modulating these interactions, are two plausible possibilities that are currently investigated in our laboratories.

Our results indicate that TRIB3 plays a central role in the mechanism of action of ABTL0812, as it has been proposed for other anti-tumoral drugs, such as THC in glioma and hepatocellular carcinoma tumors (43,44) or salinomycin in lung cancer cells (45). Interestingly, these drugs also induce autophagy -as it does ABTL0812- suggesting that TRIB3 upregulation effectively provokes a robust inhibition of the Akt/mTORC1 axis *in vivo*. THC and salinomycin exert their action by stimulation of endoplasmic reticulum stress and then activating ATF4/CHOP transcription factors that regulate TRIB3 gene. In our study, we identify a new route that links PPARα/γ activation, inhibition of Akt/mTORC1 via TRIB3 and cancer cell death.

There are contradictory reports in the literature regarding the role of TRIB3 in human cancer. Some laboratories reported elevated TRIB3 mRNA levels which correlated with bad prognosis in colorectal cancer (46) and breast cancer patients (47). On the other hand, high TRIB3 protein levels have been associated with good prognosis sensitivity to radiotherapy in breast cancer patients (48). Since TRIB3 is a very stable protein (49), the discrepancies observed between TRIB3 mRNA and protein levels in human breast cancer prognosis might be due to post-translational modifications, still to be described, that might modulate the ability of TRIB3 to interact with other proteins that regulate tumor growth. In this study, however, we show that ABTL0812 treatment induces a robust increase in TRIB3 transcription and mRNA and protein levels, which correlate

with cancer cell death and tumor growth inhibition. Our results are in agreement with a recent report showing that genetic inhibition of TRIB3 enhances tumorogenesis in different cancer models (8), and support a role for TRIB3 as a tumor suppressor.

Hyperactivation of the Akt/mTORC1 axis is observed in the majority of human cancers and blocking this pathway is an important anti-cancer strategy (5). We have shown here the activity of ABTL0812 in a panel of cancer cell lines that express high levels of phosphorylated/active Akt. Importantly, we have preliminary observed activity of ABTL0812 in patients. ABTL0812 treatment impaired Akt phosphorylation in PBMCs from patients included in the ongoing Phase I clinical trial (Fig. 6F). Therefore, Akt phosphorylation will be used as a surrogated pharmacodynamic biomarker, for estimating the recommended dose for the forthcoming Phase II trials. We have preliminarily observed increased TRIB3 mRNA levels in human PBMCs treated with ABTL0812 (Supplementary Figure 7), suggesting that TRIB3 qPCR analysis could be also used to monitor the biological activity of ABTL0812 in humans. Finally, and given its unique mechanism of action, it will be important to evaluate ABTL0812 in combination with standard chemotherapeutical compounds as well as with other target therapies. We foresee ABTL0812-based therapies will contribute to improve patients' treatment and quality of life.

Acknowledgements

The authors thank Pablo Escribá and Xavier Busquets (Universitat Illes Balears, Spain) for the preliminary identification of ABTL0812 as an anti-cancer agent (patent number WO/2010/106211). We thank Giovani Cincilla, Emiliana D'Oria and Oscar Villacañas (Intelligent Pharma SL) for *in silico* analysis, Luis Botella and Javier Soto (Medalchemy) for the synthesis of ABTL0812, and Washington Biotechnology Inc for preliminary preclinical studies. We are grateful to Victor Yuste for helpful discussions, Cristina Gutierrez for tissue culture assistance and to Servei de Genòmica i Informàtica from the UAB.

Figure Legends

Figure 1. ABTL0812 induces cancer cell death *in vitro* and reduces tumor growth in human lung and pancreatic xenografts.

A, Chemical structure of ABTL0812. **B,** ABTL0812 cell viability assays in human cancer cell lines. IC_{50} values were obtained in MTT assays after exposure to ABTL0812 for 48 h. Values are the mean ± SD of three separate determinations. **C,** LN-18 glioblastoma cells or primary rat astrocytes were incubated with ABTL0812, and 48 h later cell viability was monitored by MTT assays. Similar results were obtained in three separate determinations. **D-E,** ABTL0812 inhibits tumor growth in lung **(D)** and pancreatic **(E)** cancer xenograft models. Athymic nude mice injected with A549 or MiaPaCa-2 cells were treated with vehicle or ABTL0812 by oral gavage. Docetaxel was administered by intraperitoneal injection. Tumor growth and weight variation curves are shown. Results are the mean±SD of five mice in each group. Due to toxicity, in the docetaxel treatment only two mice were left at day 25 (n=2), and one after day 28 (n=1). *p<0.05, **p<0.01

Figure 2. ABTL0812 induces autophagy *in vitro* and *in vivo*. Autophagy mediates ABTL0812-induced cancer cell death

A, Cells were treated with 50-200 µM ABTL0812 for 12 h, lysed and levels of the autophagy-marker proteins LC3 and p62 visualized by immunoblotting. **B,** Representative electron microscopy microphotographs showing autophagosomes (right panels) in cells treated with 50µM ABTL0812 for 10h. **C,** Total protein extracted from A549 xenograft tumors (Figure 1C) were analyzed by immunoblotting for expression of LC3. Figure shows a representative analysis from vehicle (n=4) and treated (n=5) tumors. LC3-II levels were normalized with actin and estimated in densitrometric units. **D,** A549 (white columns) or MiaPaCa-2 (black columns) cells were pre-incubated with vehicle or a combination of lysosomal protease inhibitors E64d (10µM) and Pepstatin-A (PA, 10µg/mL), before treatment with 50µM ABTL0812 for 24 h. Cell viability was determined by MTT assay. Each value is the mean±SD of three different experiments. ***p<0.001 from ABTL0812 treated cells. Cells were lysed and LC3 lipidation was visualized by immunoblotting. **E,** $Atg5^{+}/^{+}$ and $Atg5^{-}/^{-}$ MEFs were treated with vehicle or ABTL0812, and cell viability determined 24 h later. Values are the mean ± SD of three different experiments. *p<0.05, ***p<0.001 from $Atg5^{+}/^{+}$ MEFs.

Figure 3. ABTL0812 inhibits the Akt/mTORC1 axis.

A549 and MiaPaCa-2 cells treated with vehicle (0) or ABTL0812 (μM) for 24h were lysed, and levels of phosphorylated proteins were analyzed by immunoblotting. Levels of total proteins and actin were used as control. Similar results were obtained in three separate experiments.

Figure 4. ABTL0812 induces PPARα and PPARγ transcriptional activities, which mediate in ABTL0812-induced cancer cell death.

A, Model for the binding of ABTL0812 (depicted in yellow) to PPARγ ligand binding domain, showing the interactions (dotted green lines) of the carboxylate and hydroxyl groups of ABTL0812 (depicted in red) with the side chains of residues (depicted in blue) within PPARγ active site. **B,** Luciferase-PPRE reporter and pRL-CMV-Renilla plasmids were co-transfected with plasmids encoding empty backbone or PPARα or PPARγ. Sixteen h post-transfection, cells were treated with vehicle or 50μM ABTL0812. 24 h later, lysates were subjected to dual-luciferase assay. Values are the mean±SD of three different experiments, each performed in triplicate and normalized using Renilla values. ***p<0.001 from cells transfected with empty plasmid. **C,** Cells were pre-incubated with vehicle (white columns), 0.2μM GW6471 (PPARα-antagonist) or 1μM GW9662 (PPARγ-antagonist) during 2 h, and then treated with 50μM ABTL0812 for 24 h. Cell viability was measured by MTT analysis. Values are the mean±SD of three different determinations. *p<0.05, ***p<0.001 from ABTL0812 treated cell.

Figure 5. ABTL0812 induces upregulation of the Akt endogenous inhibitor TRIB3 through PPARα/γ activation.

A, Cells treated with ABTL0812 for the indicated times were lysed, and levels of TRIB3 and actin analyzed by immunoblotting. **B,** Cells were transfected with luciferase-TRIB3 promoter reporter and pRL-CMV-Renilla plasmids. Sixteen h post-transfection, cells were treated with vehicle or 100 μM ABTL0812. 24 h later, lysates were subjected to dual-luciferase assay. Values are the mean±SD of three different experiments, each performed in triplicate and normalized using Renilla values. **C,** Cells were pre-incubated with vehicle or PPARα antagonist GW6471 (0.2 μM) and/or PPARγ antagonist GW9662 (1 μM) for 2 h**,** and treated for 24 h with vehicle or 50μM ABTL0812. TRIB3 mRNA levels were monitored by RT-qPCR. Values are the mean±SD of three different determinations, each performed in duplicate. ***p<0.001 from vehicle-treated cells. **D,** A549 cells were treated with PPARα agonist WY14643 (1 μM) and/or PPARγ agonist rosiglitazone (1 μM) for 24 h, lysed and proteins analyzed by immunoblotting.

Figure 6. ABTL0812-evoked TRIB3 upregulation inhibits Akt activity *in vitro* and *in vivo*.

A, Cells transfected with empty or increasing amounts of a plasmid encoding human-TRIB3 were lysed and levels of proteins monitored by immunoblotting. **B,** Immunoprecipitation of Akt from MiaPaCa-2 lysates after treatment with vehicle or ABTL0812 for 24 h. Upper panels show levels of Akt and TRIB3 in the immunoprecipitates. **C,** Wild type and TRIB3-KO MEF cells were treated with ABTL0812 for 24 h, and levels of the indicated proteins were analyzed by immunoblotting. **D,** Wild type and TRIB3-KO MEFs were treated with ABTL0812 for 24 h, and cell viability measured by MTT analysis. Values are the mean±SD of three different determinations. ***p<0.001 from TRIB3 wt. **E,** A549 and MiaPaCa-2 tumors were collected after sacrifice, and TRIB3 was evaluated by immunohistochemical analysis (left panels; scale bars: 100 μm). Levels of phospho-Akt(Ser473) were evaluated in total protein extracts, by immunoblotting (right panels). Histograms show the corresponding quantifications. *p<0.01, **p<0.005, ***p<0.001 from vehicle-treated tumors.

F, Phospho-Akt and Akt levels in PBMCs from patients before (day 0) or after 1000 mg bid ABTL0812 oral chronic treatment. Protein extracts were analyzed by immunoblotting for phospho-Akt-Ser473 and total Akt. Upper graphs show the quantification of levels of phospho-Akt normalized with Akt protein, estimated by densitometric analysis (day 1= 100%). **G,** A model showing the mechanism of action of ABTL0812.

References

1. Guertin DA and Sabatini DM. Defining the role of mTOR in cancer. Cancer Cell 2007; 12: 9-22

2. Lizcano JM and Alessi DR. The insulin signalling pathway. Curr Biol 2002; 12: R236-8

3. Hers I, Vincent EE and Tavare JM. Akt signalling in health and disease. Cell Signal 2011; 23: 1515-1527.

4. LoPiccolo J, Blumenthal GM, Bernstein WB and Dennis PA. Targeting the PI3K/Akt/mTOR pathway: effective combinations and clinical considerations. Drug Resist Updat 2008; 11: 32-50.

5. Engelman JA. Targeting PI3K signalling in cancer: opportunities, challenges and limitations. Nat Rev Cancer 2009; 9: 550-562.

6. Rodon J, Dienstmann R, Serra V and Tabernero J. Development of PI3K inhibitors: lessons learned from early clinical trials. Nat Rev Clin Oncol 2013; 10: 143-153.

7. Hirai H, Sootome H, Nakatsuru Y, Miyama K, Taguchi S, Tsujioka K, et al. MK-2206, an allosteric Akt inhibitor, enhances antitumor efficacy by standard chemotherapeutic agents or molecular targeted drugs in vitro and in vivo. Mol Cancer Ther 2010; 9: 1956-1967.

8. Salazar M, Lorente M, Garcia-Taboada E, Perez GE, Davila D, Zuniga-Garcia P, et al. Loss of Tribbles pseudokinase-3 promotes Akt-driven tumorigenesis via FOXO inactivation. Cell Death Differ 2015; 22: 131-144.

9. Erazo T, Moreno A, Ruiz-Babot G, Rodriguez-Asiain A, Morrice NA, Espadamala J, et al. Canonical and kinase activity-independent mechanisms for extracellular signal-regulated kinase 5 (ERK5) nuclear translocation require dissociation of Hsp90 from the ERK5-Cdc37 complex. Mol Cell Biol 2013; 33: 1671-1686.

10. Rodriguez-Asiain A, Ruiz-Babot G, Romero W, Cubi R, Erazo T, Biondi RM, et al. Brain specific kinase-1 BRSK1/SAD-B associates with lipid rafts: modulation of kinase activity by lipid environment. Biochim Biophys Acta 2011; 1811: 1124-1135.

11. Lizcano JM, Alrubaie S, Kieloch A, Deak M, Leevers SJ and Alessi DR. Insulin-induced Drosophila S6 kinase activation requires phosphoinositide 3-kinase and protein kinase B. Biochem J 2003; 374: 297-306.

12. Salazar M, Carracedo A, Salanueva IJ, Hernandez-Tiedra S, Egia A, Lorente M, et al. Cannabinoid action induces autophagy-mediated cell death through stimulation of ER stress in human glioma cells. Autophagy 2009; 5: 1048-1049.

13. Klionsky DJ, Abdalla FC, Abeliovich H, Abraham RT, Acevedo-Arozena A, Adeli K, et al. Guidelines for the use and interpretation of assays for monitoring autophagy. Autophagy 2012; 8: 445-544.

14. Virgin HW and Levine B. Autophagy genes in immunity. Nat Immunol 2009; 10: 461-470.

15. Yang ZJ, Chee CE, Huang S and Sinicrope FA. The role of autophagy in cancer: therapeutic implications. Mol Cancer Ther 2011; 10: 1533-1541.

16. Maggiora GM and Shanmugasundaram V. Molecular similarity measures. Methods Mol Biol 2011; 672, 39-100.

17. Xiao B, Su M, Kim EL, Hong J, Chung HY, Kim HS, et al. Synthesis of PPARγ activators inspired by the marine natural product, paecilocin A. Mar Drugs 2014; 12: 926-939.

18. Koo SH, Satoh H, Herzig S, Lee CH, Hedrick S, Kulkarni R, et al. PGC-1 promotes insulin resistance in liver through PPAR-alpha-dependent induction of TRB-3. Nat Med 2004; 10: 530-534.

19. Du K, Herzig S, Kulkarni RN and Montminy M. TRB3: a tribbles homolog that inhibits Akt/PKB activation by insulin in liver. Science 2003, 300: 1574-1577.

20. Galluzzi L, Pietrocola F, Bravo-San Pedro JM, Amaravadi RK, Baehrecke EH, Cecconi F, et al. Autophagy in malignant transformation and cancer progression. EMBO J 2015; 34: 856-880.

21. Rovito D, Giordano C, Vizza D, Plastina P, Barone I, Casaburi I, et al. Omega-3 PUFA ethanolamides DHEA and EPEA induce autophagy through PPARγ activation in MCF-7 breast cancer cells. J Cell Physiol 2013; 228: 1314-1322.

22. Shinohara H, Taniguchi K, Kumazaki M, Yamada N, Ito Y, Otsuki Y, et al. T Anti-cancer fatty-acid derivative induces autophagic cell death through modulation of PKM isoform expression profile mediated by bcr-abl in chronic myeloid leukemia. Cancer Lett 2015; 360: 28-38.

23. Marcilla-Etxenike A, Martin ML, Noguera-Salva MA, Garcia-Verdugo JM, Soriano-Navarro M, Dey I, et al. 2-Hydroxyoleic acid induces ER stress and autophagy in various human glioma cell lines. PLoS One 2012; 7: e48235.

24. Holohan C, Van SS, Longley DB and Johnston PG. Cancer drug resistance: an evolving paradigm. Nat Rev Cancer 2013; 13: 714-726.

25. Sui X, Chen R, Wang Z, Huang Z, Kong N, Zhang M, et al. Autophagy and chemotherapy resistance: a promising therapeutic target for cancer treatment. Cell Death Dis 2013; 4: e838.

26. Hu M, Huang H, Zhao R, Li P, Li M, Miao H, et al. AZD8055 induces cell death associated with autophagy and activation of AMPK in hepatocellular carcinoma. Oncol Rep 2014; 31: 649-656.

27. Zhang H, Berel D, Wang Y, Li P, Bhowmick NA, Figlin RA, et al. A comparison of Ku0063794, a dual mTORC1 and mTORC2 inhibitor, and temsirolimus in preclinical renal cell carcinoma models. PLoS One 2013; 8: e54918.

28. Lin CI, Whang EE, Donner DB, Du J, Lorch J, He F, et al. Autophagy induction with RAD001 enhances chemosensitivity and radiosensitivity through Met inhibition in papillary thyroid cancer. Mol Cancer Res 2010; 8: 1217-1226.

29. Li AC and Palinski W. Peroxisome proliferator-activated receptors: how their effects on macrophages can lead to the development of a new drug therapy against atherosclerosis. Annu Rev Pharmacol Toxicol 2006; 46: 1-39.

30. Wang L, Waltenberger B, Pferschy-Wenzig EM, Blunder M, Liu X, Malainer C, et al. Natural product agonists of peroxisome proliferator-activated receptor gamma (PPARγ): a review. Biochem Pharmacol 2014; 92: 73-89.

31. Ferre P. The biology of peroxisome proliferator-activated receptors: relationship with lipid metabolism and insulin sensitivity. Diabetes 2004; 53 Suppl 1: S43-S50.

32. Shen B, Chu ES, Zhao G, Man K, Wu CW, Cheng JT, et al. PPARgamma inhibits hepatocellular carcinoma metastases in vitro and in mice. Br J Cancer 2012; 106: 1486-1494.

33. Panigrahy D, Kaipainen A, Huang S, Butterfield CE, Barnes CM, Fannon M, et al. PPARalpha agonist fenofibrate suppresses tumor growth through direct and indirect angiogenesis inhibition. Proc Natl Acad Sci U S A 2008; 105: 985-990.

34. Bishop-Bailey D. PPARs and angiogenesis. Biochem Soc Trans 2011; 39: 1601-1605.

35. Li T, Zhang Q, Zhang J, Yang G, Shao Z, Luo J, et al. Fenofibrate induces apoptosis of triple-negative breast cancer cells via activation of NF-κB pathway. BMC Cancer 2014; 14: 96.

36. Zang C, Liu H, Bertz J, Possinger K, Koeffler HP, Elstner E, et al. Induction of endoplasmic reticulum stress response by TZD18, a novel dual ligand for peroxisome proliferator-activated receptor alpha/gamma, in human breast cancer cells. Mol Cancer Ther 2009; 8: 2296-2307.

37. Hegedus Z, Czibula A and Kiss-Toth E. Tribbles: novel regulators of cell function; evolutionary aspects. Cell Mol Life Sci 2006; 63: 1632-1641.

38. Grosshans J and Wieschaus E. A genetic link between morphogenesis and cell division during formation of the ventral furrow in Drosophila. Cell 2000; 101: 523-531.

39. Hua F, Mu R, Liu J, Xue J, Wang Z, Lin H, et al. TRB3 interacts with SMAD3 promoting tumor cell migration and invasion. J Cell Sci 2011; 124: 3235-3246.

40. Ohoka N, Yoshii S, Hattori T, Onozaki K and Hayashi H. TRB3, a novel ER stress-inducible gene, is induced via ATF4-CHOP pathway and is involved in cell death. EMBO J 2005; 24: 1243-1255.

41. Kiss-Toth E, Bagstaff SM, Sung HY, Jozsa V, Dempsey C, Caunt JC, et al. Human tribbles, a protein family controlling mitogen-activated protein kinase cascades. J Biol Chem 2004; 279: 42703-42708.

42. Liu J, Zhang W, Chuang GC, Hill HS, Tian L, Fu Y, et al. Role of TRIB3 in regulation of insulin sensitivity and nutrient metabolism during short-term fasting and nutrient excess. Am J Physiol Endocrinol Metab 2012; 303: E908-E916.

43. Salazar M, Carracedo A, Salanueva IJ, Hernandez-Tiedra S, Lorente M, Egia A, et al. Cannabinoid action induces autophagy-mediated cell death through stimulation of ER stress in human glioma cells. J Clin Invest 2009; 119: 1359-1372.

44. Vara D, Salazar M, Olea-Herrero N, Guzman M, Velasco G and Diaz-Laviada I. Anti-tumoral action of cannabinoids on hepatocellular carcinoma: role of AMPK-dependent activation of autophagy. Cell Death Differ 2011; 18: 1099-1111

45. Li T, Su L, Zhong N, Hao X, Zhong D, Singhal S, et al. Salinomycin induces cell death with autophagy through activation of endoplasmic reticulum stress in human cancer cells. Autophagy 2013; 9: 1057-1068.

46. Miyoshi N, Ishii H, Mimori K, Takatsuno Y, Kim H, Hirose H, et al. Abnormal expression of TRIB3 in colorectal cancer: a novel marker for prognosis. Br J Cancer 2009; 101: 1664-1670.

47. Wennemers M, Bussink J, Scheijen B, Nagtegaal ID, van Laarhoven HW, Raleigh JA, et al. Tribbles homolog 3 denotes a poor prognosis in breast cancer and is involved in hypoxia response. Breast Cancer Res 2011b; 13: R82.

48. Wennemers M, Bussink J, Grebenchtchikov N, Sweep FC and Span PN. TRIB3 protein denotes a good prognosis in breast cancer patients and is associated with hypoxia sensitivity. Radiother Oncol 2011a; 101: 198-202.

49. Wennemers M, Bussink J, van den BT, Sweep FC and Span PN. Regulation of TRIB3 mRNA and protein in breast cancer. PLoS One 2012; 7: e49439.

A

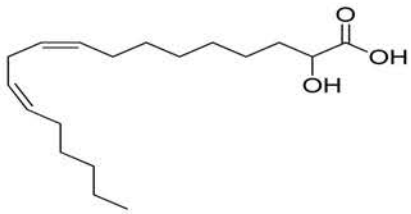

B

Cancer cell line	IC50 ± SD
PC3 (prostate adenocarcinoma)	22 ± 2 μM
MiaPaCa-2 (pancreatic adenocarcinoma)	54 ± 2 μM
A549 (lung adenocarcinoma)	62 ± 5 μM
LN18 (glioblastoma)	20 ± 2 μM
SK-BR3 (breast adenocarcinoma)	23 ± 1 μM
Hec1A (endometrial adenocarcinoma)	32 ± 4 μM

C

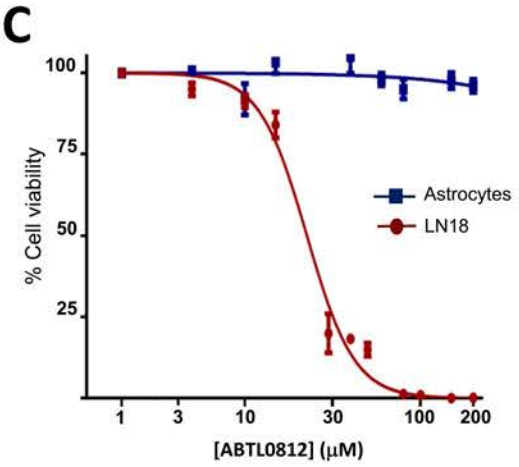

D

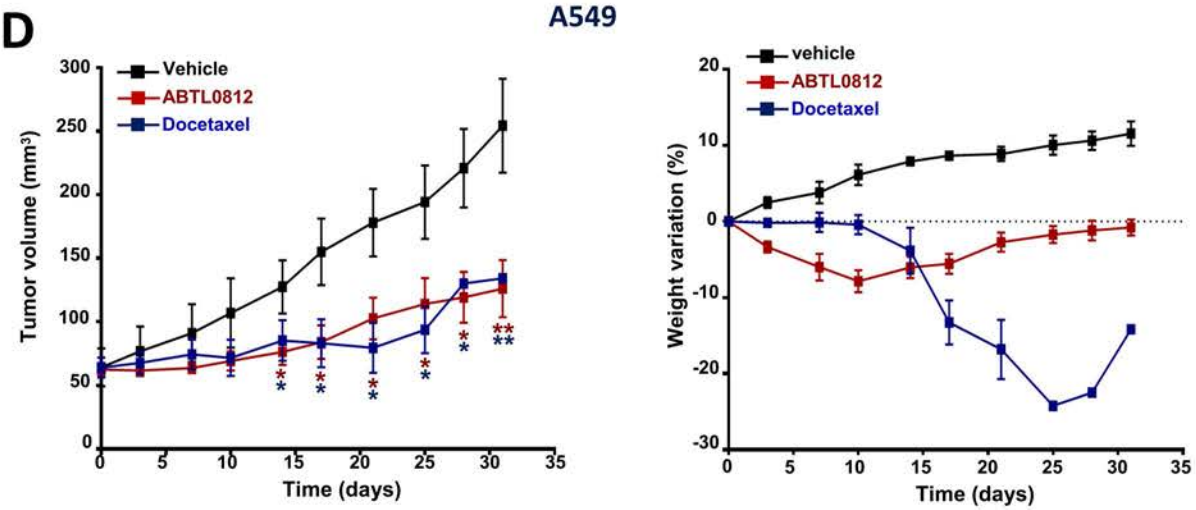

E

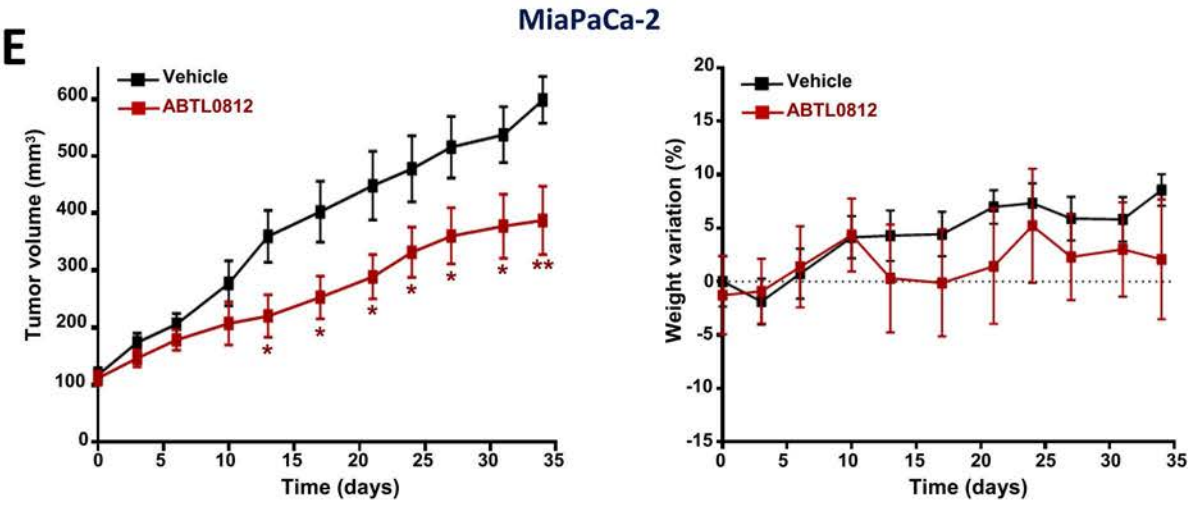

Figure 1

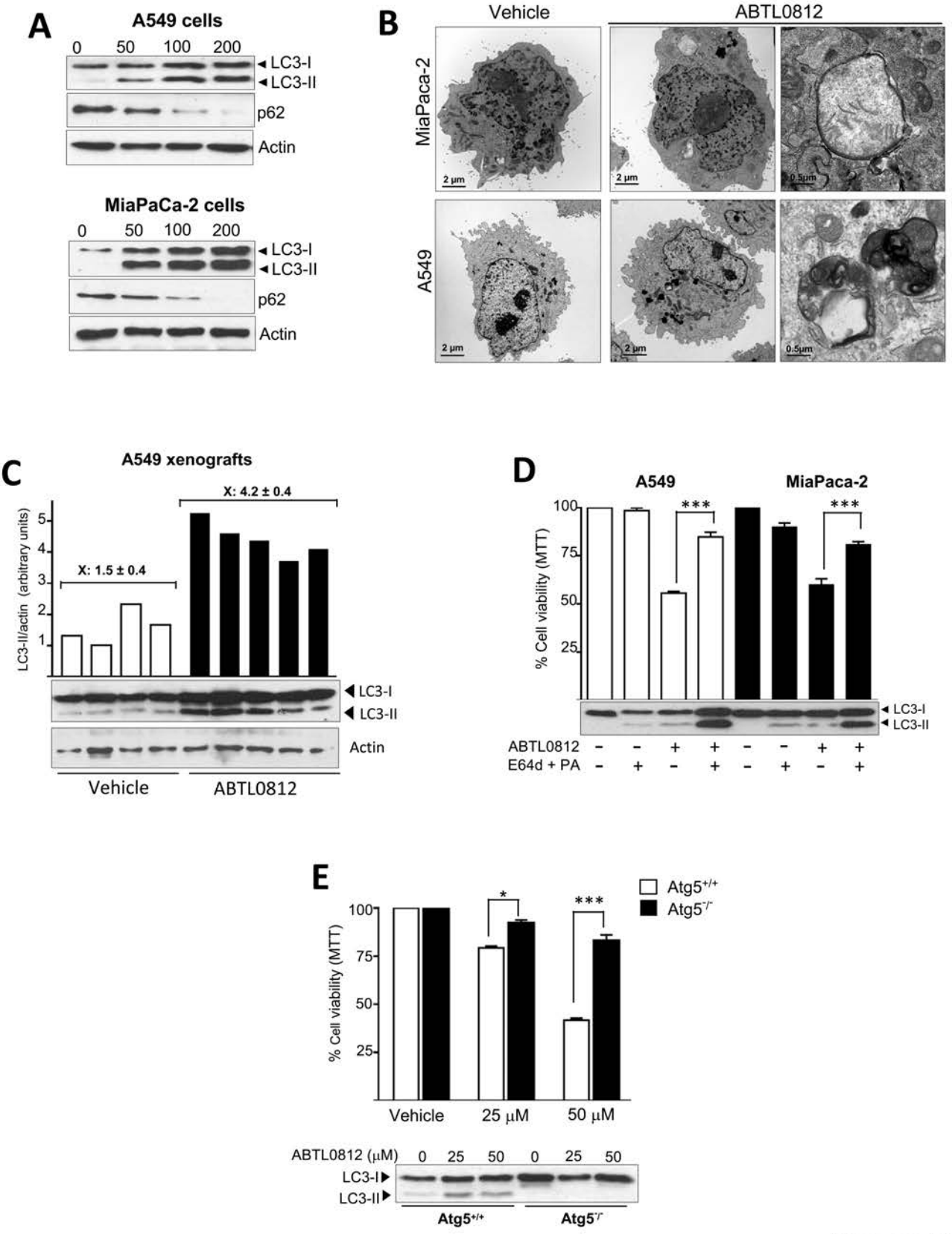

Figure 2

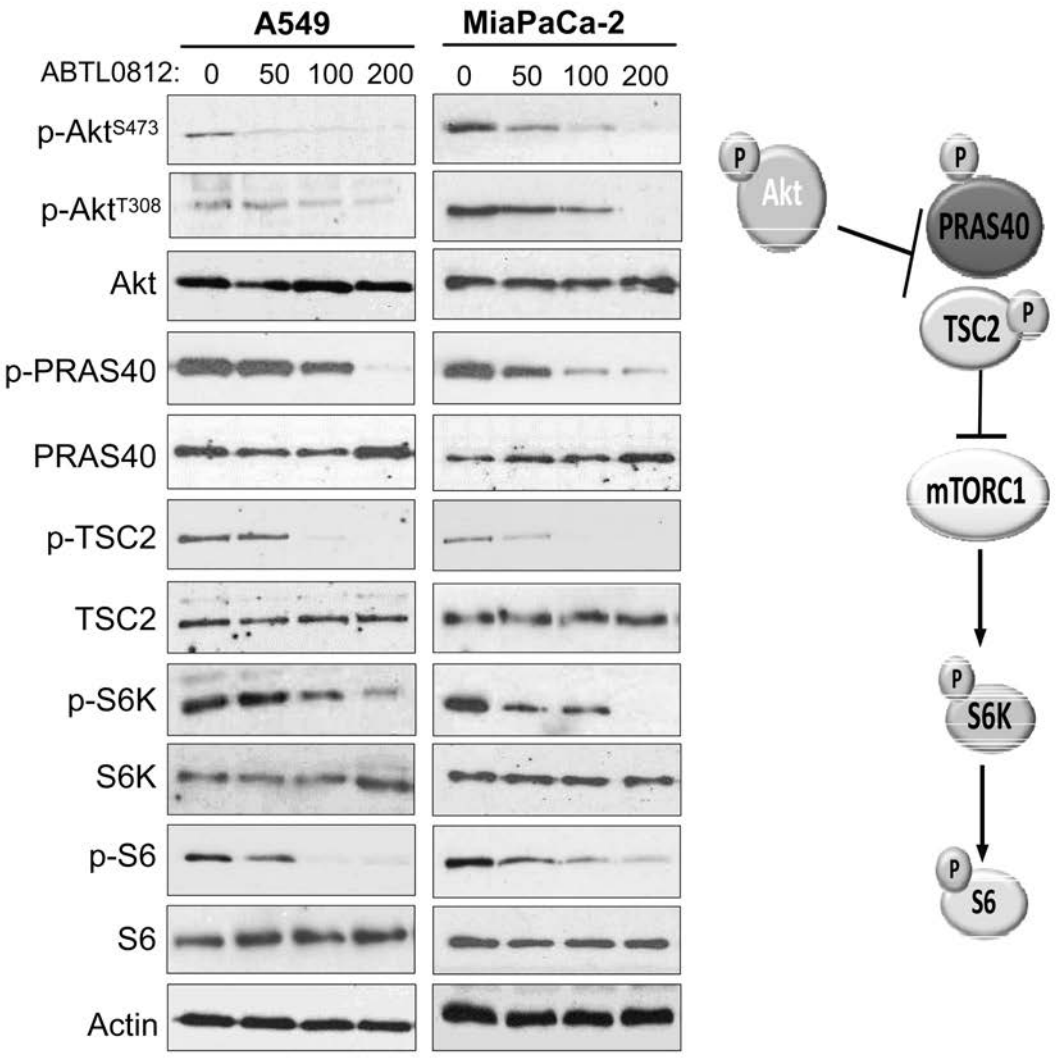

Figure 3

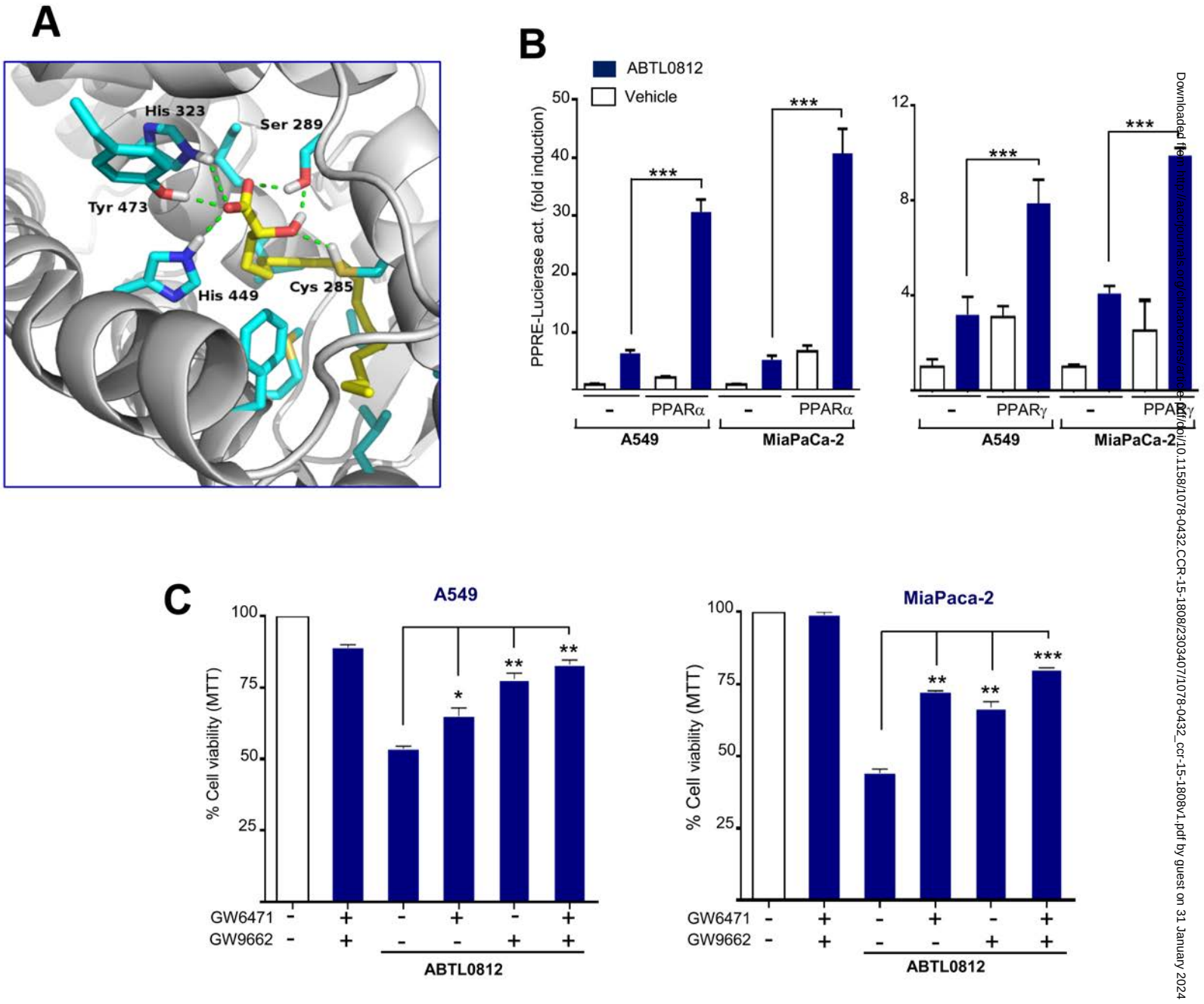

Figure 4

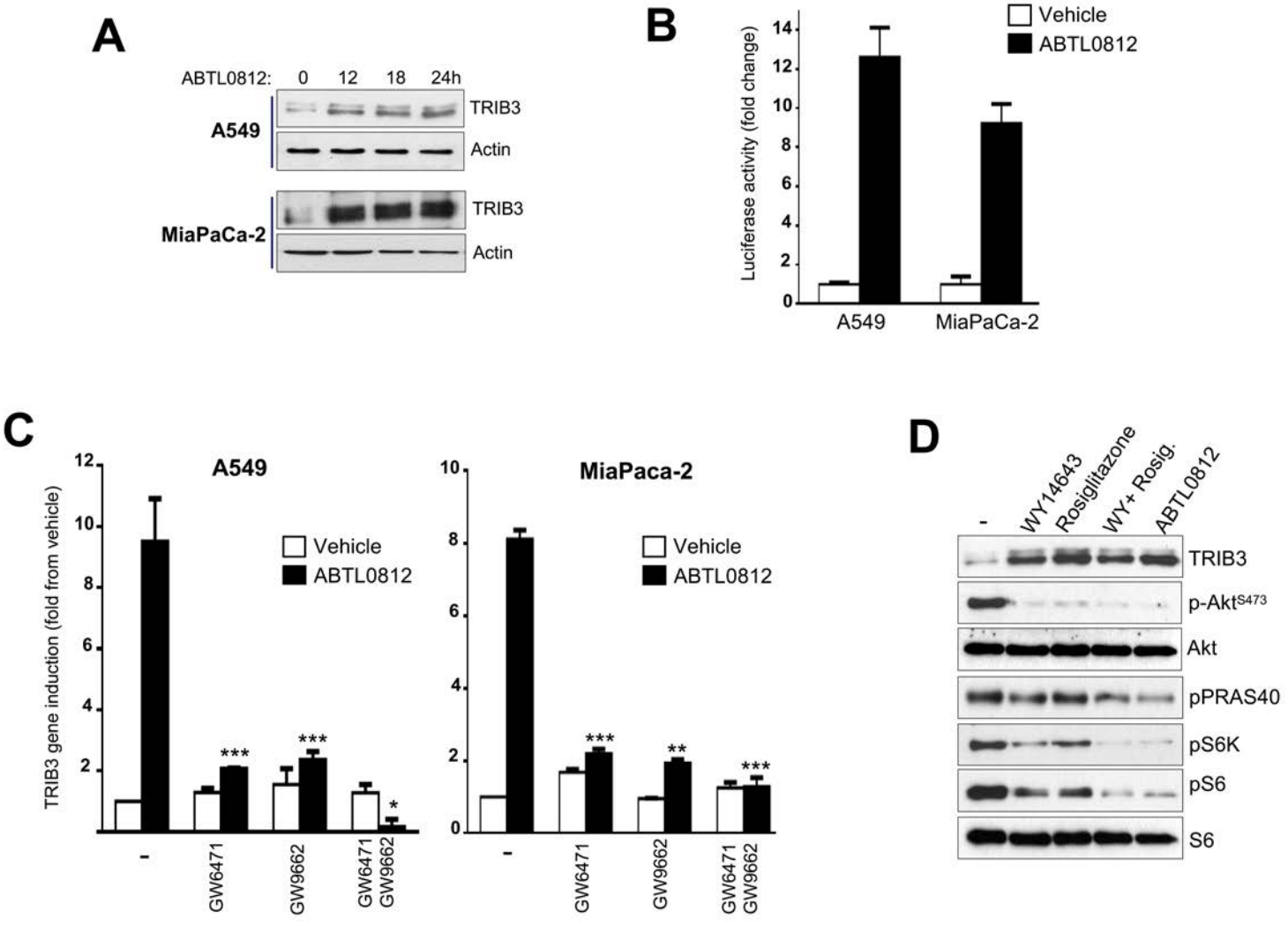

Figure 5

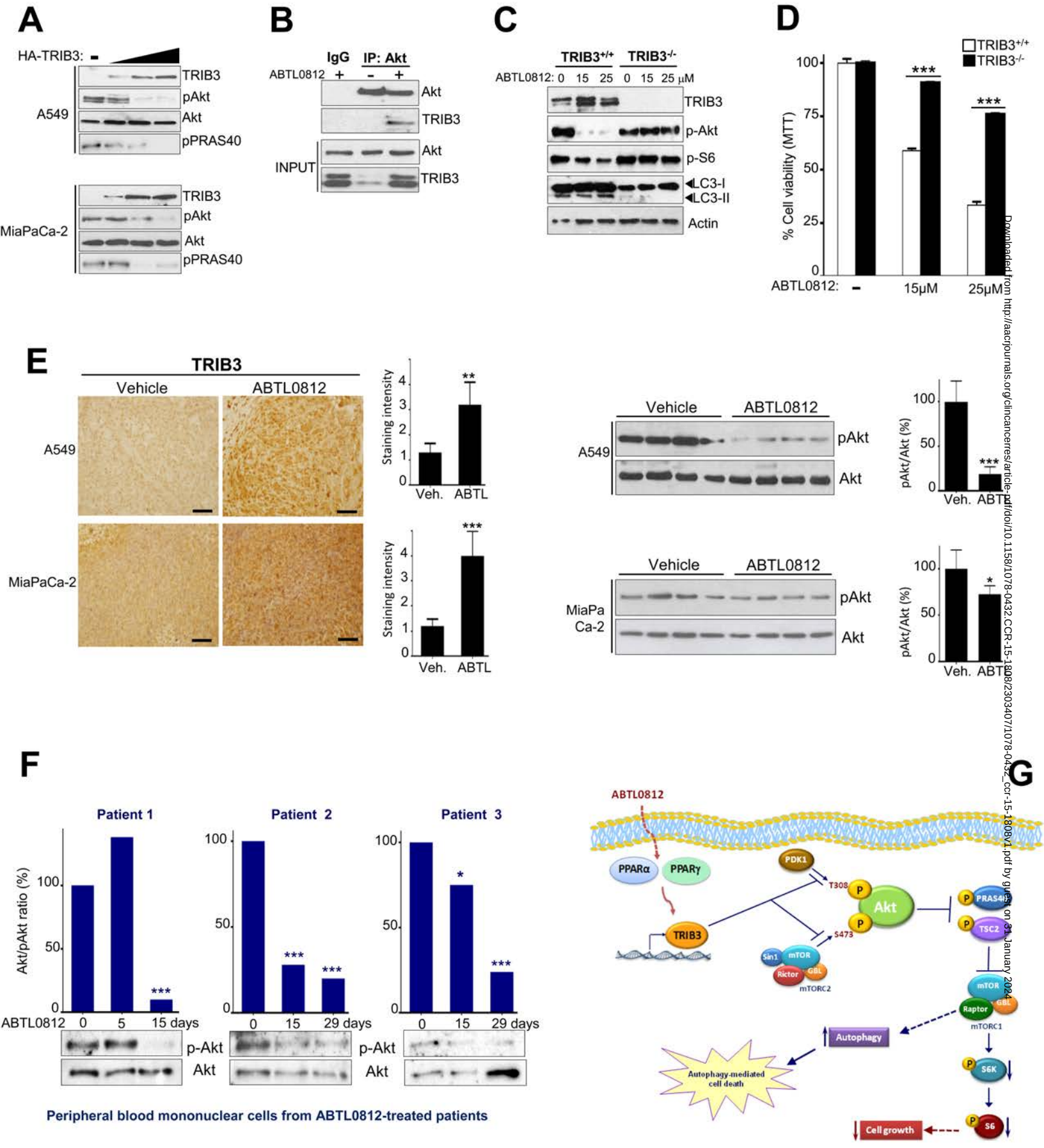

Figure 6